EMBEDDED TRAPPED MODES FOR OBSTACLES IN TWO-DIMENSIONAL WAVEGUIDES

by M. McIVER, C. M. LINTON, P. McIVER, J. ZHANG

(*Department of Mathematical Sciences, Loughborough University, Loughborough, Leicestershire* LE11 3TU)

and R. PORTER

(*School of Mathematics, University of Bristol, Bristol* BS8 1TW)

[Received 18 February 2000]

Summary

In this paper we investigate the existence of embedded trapped modes for symmetric obstacles which are placed on the centreline of a two-dimensional acoustic waveguide. Modes are sought which are antisymmetric about the centreline of the channel but which have frequencies that are above the first cut-off for antisymmetric wave propagation down the guide. In the terminology of spectral theory this means that the eigenvalue associated with the trapped mode is embedded in the continuous spectrum of the relevant operator.

A numerical procedure based on a boundary integral technique is developed to search for embedded trapped modes for bodies of general shape. In addition two approximate solutions for trapped modes are found; the first is for long plates on the centreline of the channel and the second is for slender bodies which are perturbations of plates perpendicular to the guide walls. It is found that embedded trapped modes do not exist for arbitrary symmetric bodies but if an obstacle is defined by two geometrical parameters then branches of trapped modes may be obtained by varying both of these parameters simultaneously. One such branch is found for a family of ellipses of varying aspect ratio and size. The thin plates which are parallel and perpendicular to the guide walls are found to correspond to the end points of this branch.

1. Introduction

The existence of trapped modes in acoustic waveguides, water-wave channels and in the vicinity of electromagnetic gratings is now well established. Although physically distinct, the mathematical representations of these modes in their different contexts have many similarities. For example, once the depth and time dependence have been removed from the problem, a trapped mode in a water-wave channel of constant depth which contains a vertical cylinder of uniform cross-section is mathematically equivalent to an acoustic trapped mode in a two-dimensional waveguide with rigid walls which contains an obstacle whose shape is given by the cross-section of the cylinder. Both correspond to non-zero solutions of the two-dimensional Helmholtz equation which satisfy homogeneous Neumann conditions on the walls and body boundary and have finite energy. Such modes have been proven to exist by Evans *et al.* (**1**) for a fairly general class of cylinders which have a line of symmetry and are symmetrically placed about the centreline of the channel. More recently

Khallaf *et al.* (**2**) proved that a symmetrically placed, rectangular obstacle with sides of length $2a$ parallel to the guide and $2b$ perpendicular to the guide may support more than one trapped mode, and that the number of trapped modes increases with a.

If no restrictions are placed on the symmetry of the solutions then the trapped modes occur at frequencies that correspond to eigenvalues which are embedded in the continuous spectrum of the relevant operator. However, if the structure is symmetric about the centreline of the channel and the motion is split into symmetric and antisymmetric parts then the operator may be decomposed so that the essential spectrum of the antisymmetric part has a non-zero lower limit and the trapped mode corresponds to an eigenvalue which is below this value. (The square root of this lower limit is called the 'cut-off' because it represents the value of the non-dimensional wave number below which waves that are antisymmetric about the channel centreline cannot propagate down the guide.) In this case standard variational methods may be used to prove the existence of an antisymmetric trapped mode. However, Evans *et al.* (**3**) also found that trapped modes exist for flat plates which are parallel to the guide walls, irrespective of whether the plate is on the centreline of the guide. In the latter case it is not possible to decompose the operator into symmetric and antisymmetric parts, but Davies and Parnovski (**4**) and Groves (**5**) independently showed that it is possible to decompose the operator in an alternative fashion so that the trapped mode corresponds to an eigenvalue below the cut-off of an appropriate operator. Their results also prove the existence of trapped modes for thin obstacles aligned with the guide walls in higher dimensions. Further extensions to higher dimensions have been made by Linton and McIver (**6**), who showed that trapped modes exist for axisymmetric bodies in cylindrical waveguides by exploiting the symmetry of the problem and looking for modes which have a specific azimuthal variation.

Recently Evans and Porter (**7**) have provided numerical evidence for the existence of an isolated trapped mode in the presence of a circular obstacle on the centreline of a two-dimensional guide, above the cut-off for antisymmetric wave propagation in the guide. The trapped mode exists only for one circle with a particular radius and it is embedded in the continuous spectrum of the antisymmetric operator. The purpose of the present work is to show numerically that rather than being isolated, this mode is one of a continuous branch which exists for ellipses of varying aspect ratio. The branch of modes begins with a trapped mode for a flat plate aligned parallel to the walls of the guide and ends with a standing wave for a flat plate which is perpendicular to the guide walls. Approximate and exact expressions are derived in section 3 and section 4 respectively for the lengths of these plates and the trapped mode frequencies associated with them. In addition the mode found by Evans and Porter (**7**) is shown to be a point on a branch of modes which exists for hypercircles, that is, obstacles with shape $|x/a|^\nu + |y/a|^\nu = 1$, $-a \leqslant x \leqslant a$, where x is measured along the guide, y is measured across the guide and a and ν vary along the branch. Theoretically ν may take any positive value but in practice calculations were not performed for $\nu < 1$ because of numerical difficulties. The other end of the branch ($\nu \to \infty$) corresponds to a square and the trapped mode will be shown to tend to a standing wave in this limit.

Although computations are performed only for ellipses and hypercircles, it is expected that a curve of trapped modes exists at wave numbers above the first cut-off for any two-parameter family of sufficiently smooth obstacles which are symmetric in both x and y and which contain the Evans and Porter circle. This is in contrast to the situation below the cut-off where trapped modes exist for all (sufficiently smooth) bodies which are symmetric in y, irrespective of any symmetry in x. In the latter case symmetry in x is not required, as there can be no propagation of waves to either infinity. In the former case, however, the wave field is different at either infinity if the body has no symmetry in x. In this situation it is anticipated that an extra geometrical parameter needs to be

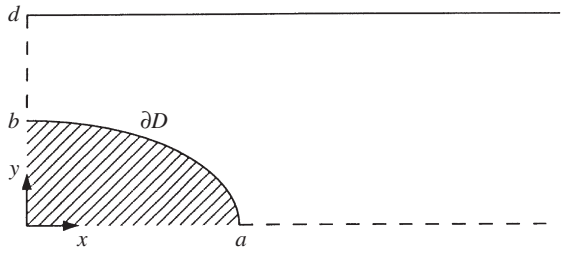

Fig. 1 Definition sketch

varied to ensure that the wave field decays at both infinities and a trapped mode exists. At wave numbers both above and below the cut-off symmetry of the geometry in y is necessary to allow motion which is only antisymmetric in y to be considered.

The approximate theory developed in section 3 predicts that there are a countably infinite number of plates aligned parallel to the walls which can support trapped modes and a proof of this result for sufficiently long plates is given in the appendix. Each one of these plates may be deformed into an ellipse or a body of different shape for which trapped modes exist. Future work will investigate the structure of these branches in detail for the case where the deformed obstacles are rectangular blocks.

2. Formulation

The problem is formulated for an arbitrary, doubly-symmetric body on the centreline of a two-dimensional channel. As has already been discussed, the symmetry of the body in both x and y is crucial for what follows. A quarter-section of the guide is illustrated in Fig. 1. As the body has two lines of symmetry a trapped mode potential ϕ may be sought which is symmetric in x and antisymmetric in y. Thus ϕ satisfies

$$(\nabla^2 + k^2)\phi = 0 \tag{1}$$

in the guide exterior to the body and is subject to the boundary conditions

$$\phi = 0 \quad \text{on} \quad y = 0, \quad x > a, \tag{2}$$

$$\frac{\partial \phi}{\partial y} = 0 \quad \text{on} \quad y = d, \quad x > 0, \tag{3}$$

$$\frac{\partial \phi}{\partial x} = 0 \quad \text{on} \quad x = 0, \quad b < y < d, \tag{4}$$

$$\frac{\partial \phi}{\partial n} = 0 \quad \text{on} \quad \partial D, \tag{5}$$

and

$$\phi \to 0 \quad \text{as} \quad x \to \infty. \tag{6}$$

In the above, $\partial/\partial n$ denotes differentiation in the direction normal to the body boundary ∂D. The work of Evans *et al.* (**1**) proves that at least one trapped mode exists for a large class of obstacles provided that $kd < \pi/2$. The aim here is to seek obstacles which support trapped modes for values of kd in the range $\pi/2 < kd < 3\pi/2$, the upper limit being the infimum of the set of values of kd for which antisymmetric waves of the form $e^{i\alpha x} \sin 3\pi y/2d$, $9\pi^2/4d^2 + \alpha^2 = k^2$ can propagate down the guide. In particular it will be shown numerically that trapped modes exist for elliptical obstacles of the form $(x/a)^2 + (y/b)^2 = 1$. Modes will be found for a range of values of b/d, but for each value of b/d modes will only be found for a discrete set of values of a/d. The values of kd for all the modes lie in the range $\pi < kd < 3\pi/2$ and a physical explanation of this last result is given in the next section. In addition to the ellipses, embedded trapped modes will be found for shapes of the form $|x/a|^\nu + |y/a|^\nu = 1$ for values of $\nu \geqslant 1$.

The numerical method employed to determine the trapped mode frequencies uses ideas of Evans and Porter (**7**). A complex, homogeneous integral equation is set up for the trapped mode potential ϕ under the assumption that ϕ satisfies (6). This is split into real and imaginary parts and the resulting equations are discretized numerically. A non-zero solution for ϕ which decays at infinity is possible if the determinant of the real matrix is zero and if the eigenvector of this matrix which corresponds to the zero eigenvalue satisfies the imaginary part of the equation. The latter is regarded as a side condition which ϕ must satisfy.

The Green's function, $G(x, y; \xi, \eta)$, which represents the potential at (x, y) due to a source at (ξ, η) in an empty quarter-guide and which is symmetric in y and antisymmetric in x satisfies

$$(\nabla^2 + k^2)G = -\delta(x - \xi)\delta(y - \eta) \tag{7}$$

in the guide,

$$G = 0 \quad \text{on} \quad y = 0, \tag{8}$$

$$\frac{\partial G}{\partial y} = 0 \quad \text{on} \quad y = d \tag{9}$$

and

$$\frac{\partial G}{\partial x} = 0 \quad \text{on} \quad x = 0, \tag{10}$$

where $\delta(\cdot)$ is the Dirac delta function. Furthermore G is required to behave like outgoing waves as $|x - \xi| \to \infty$. Linton and Evans (**8**) showed that one representation of G is given by

$$\begin{aligned} G = {} & \tfrac{1}{4}[Y_0(kr) + Y_0(kr_1) + Y_0(kr_2) + Y_0(kr_3)] \\ & + \frac{2}{\pi} \operatorname{Re} \int_0^\infty \frac{e^{-k\gamma d}}{\gamma \cosh k\gamma d} \cosh k\gamma(d - y) \cos kxt \cos k\xi t \, \mathrm{d}t \\ & - \frac{2i}{kd} \sum_{n=1}^{j_a} \frac{1}{\tau_n} \sin(n - \tfrac{1}{2}) \frac{\pi y}{d} \sin(n - \tfrac{1}{2}) \frac{\pi \eta}{d} \cos kx\tau_n \cos k\xi\tau_n, \end{aligned} \tag{11}$$

where

$$r = [(x-\xi)^2 + (y-\eta)^2]^{1/2}, \tag{12}$$

$$r_1 = [(x-\xi)^2 + (y+\eta-2d)^2]^{1/2}, \tag{13}$$

$$r_2 = [(x+\xi)^2 + (y-\eta)^2]^{1/2}, \tag{14}$$

$$r_3 = [(x+\xi)^2 + (y+\eta-2d)^2]^{1/2}, \tag{15}$$

$$\gamma(t) = \begin{cases} -i(1-t^2)^{1/2}, & t \leqslant 1, \\ (t^2-1)^{1/2}, & t > 1, \end{cases} \tag{16}$$

$$\tau_n = [1 - ((n-\tfrac{1}{2})\pi/kd)^2]^{1/2} \tag{17}$$

and j_a is the integer chosen to satisfy

$$(j_a - \tfrac{1}{2})\pi < kd < (j_a + \tfrac{1}{2})\pi. \tag{18}$$

If $kd < \pi/2$ then from (18) $j_a = 0$ and it follows from (11) that the Green's function is purely real and decays at infinity. This means that a real integral equation may be developed to search for trapped modes in this frequency range and this was the method used by Linton and Evans (**8**). However, if $\pi/2 < kd < 3\pi/2$ then $j_a = 1$ and there is one term in the series part of G. In this case the Green's function is complex and behaves like outgoing waves as $|x-\xi| \to \infty$. In particular

$$\mathrm{Im}[G] = -\frac{2}{kd\tau_1} \sin\frac{\pi y}{2d} \sin\frac{\pi\eta}{2d} \cos k\xi\tau_1 \cos kx\tau_1 = G_1(x,y)G_1(\xi,\eta). \tag{19}$$

Application of Green's theorem to the trapped mode potential ϕ and G yields the integral equation

$$\tfrac{1}{2}\phi(x,y) = \int_{\partial D} \phi(\xi,\eta) \frac{\partial G}{\partial n}(x,y;\xi,\eta)\,\mathrm{d}s, \tag{20}$$

where ∂D is the boundary of the body in the region $x \geqslant 0$, $y \geqslant 0$, (x, y) is a point on the cylinder surface and $\partial G/\partial n$ is the inward normal derivative of G to the body with respect to the variables (ξ, η).

The integral equation in (20) is known to be singular at certain values of kd, called 'irregular values'. These are values at which there are non-zero solutions of the Helmholtz equation in the interior of the body, which satisfy Dirichlet conditions on ∂D and $y = 0$ and a Neumann condition on $x = 0$. The irregular values do not correspond to trapped modes but are merely an artefact of the mathematical formulation of the problem. However, they can give rise to spurious indications of trapped modes and need to be avoided in any computational scheme. For a body which is contained within a rectangle of depth $2b$ and width $2a$ Courant and Hilbert (**9**, Chapter VI, section 2) showed that the lowest such value satisfies

$$kd \geqslant \pi d\left(\frac{1}{4a^2} + \frac{1}{b^2}\right)^{1/2} \geqslant \frac{\pi d}{b}. \tag{21}$$

It will be shown in section 5 that all of the ellipses for which trapped modes were found satisfy $b/d < \frac{1}{2}$ and so from (21) any irregular value for this geometry satisfies $kd > 2\pi$ which is outside the range of interest. Furthermore any obstacle of the form $|x/a|^\nu + |y/a|^\nu = 1$ which supports

trapped modes was found to have $a/d = b/d \leqslant \frac{1}{2}$ for $\nu \geqslant 1$. In this case the same bound on the irregular frequencies applies.

Without loss of generality the function ϕ is assumed to be real and so (20) reduces to the two equations

$$\tfrac{1}{2}\phi(x, y) = \int_{\partial D} \phi(\xi, \eta) \frac{\partial}{\partial n} [\mathrm{Re}[G(x, y; \xi, \eta))]] \, \mathrm{d}s \tag{22}$$

and

$$\int_{\partial D} \phi(\xi, \eta) \frac{\partial}{\partial n} [\mathrm{Im}[G(x, y; \xi, \eta))]] \, \mathrm{d}s = 0. \tag{23}$$

The boundary of the body is described in terms of the angle θ which is measured anticlockwise from the x-axis and so $0 \leqslant \theta \leqslant \pi/2$ for the quarter-body. The normal derivative of the Green's function is well behaved at all points on the body except when $(x, y) = (\xi, \eta)$, where it is undefined. However, the limiting values of the derivative on either side of this point exist and are equal, and so it is the limit that is used in the computational scheme where necessary. The integration in (22) and (23) is performed using Gauss–Legendre quadrature and the expression in (22) is evaluated at the corresponding quadrature points. This yields the matrix system of equations

$$\sum_{j=1}^{M} A_{ij} \phi_j = 0, \tag{24}$$

where

$$A_{ij} = \tfrac{1}{2}\delta_{ij} - w_j \frac{\partial}{\partial n} [\mathrm{Re}[G(x(\theta_i), y(\theta_i); \xi(\theta_j), \eta(\theta_j))]] \left(\frac{\mathrm{d}s}{\mathrm{d}\theta} \right)_{\theta = \theta_j}, \tag{25}$$

δ_{ij} is the Kronecker delta, $\phi_j = \phi(x(\theta_j), y(\theta_j))$ and θ_i and w_i, $i = 1, \ldots, M$ are the Gauss–Legendre quadrature points and weight functions respectively given by Abramowitz and Stegun (**10**, equation 25.4.29). The elements A_{ij} need to be calculated numerically and this involves many computations of the Green's function. Linton (**11**) has developed analytical representations for G which lead to numerical algorithms that are much more efficient than an algorithm which computes G directly from (11) and these efficient algorithms were used in the present calculations. From (19) and (23) the imaginary part of the equation may be discretized to give the side condition

$$S = \sum_{j=1}^{M} \phi_j w_j \frac{\partial}{\partial n} \left[\sin \frac{\pi \eta}{2d} \cos k\xi\tau_1 \right]_{(\eta,\xi)=(\eta(\theta_j),\xi(\theta_j))} \left(\frac{\mathrm{d}s}{\mathrm{d}\theta} \right)_{\theta=\theta_j} = 0. \tag{26}$$

The system of equations in (24) has a non-trivial solution for ϕ when $\det(A) = 0$. However, this solution only corresponds to a trapped mode if the resulting function ϕ satisfies the side condition (26). If the geometry were symmetric in y but not in x then the resulting Green's function would not be symmetric in x and the far-field form of its imaginary part would not be expressible as the product of a function of (x, y) and a function of (ξ, η) as in (19) but would be the sum of two separable terms instead. This would lead to two side conditions which need to be satisfied rather than one and in general an additional geometrical parameter would have to be varied in the search for trapped modes.

The numerical procedure used to determine where a trapped mode exists is as follows. For a fixed geometrical parameter (for example, b/d or ν) the curve on which $\det(A) = 0$ is plotted is the $(a/d, kd)$-plane. A normalized eigenfunction $\{\phi_j\}$ and the corresponding value of S are calculated from (24) and (26) at each point on the curve in such a way that they vary smoothly along the curve. Points at which S changes sign correspond to trapped modes. (In principle either $\det(A)$ or S could equal zero without changing sign but it would be impossible to demonstrate this numerically. In practice, however, both quantities changed sign near any zero.) This method is based on that used by Evans and Porter (**7**) and although it does not require the introduction of the function $\tilde{S}$ used in their paper, it is believed to be as robust numerically. The equivalent function $\tilde{S}$ to that used by Evans and Porter (**7**) is

$$\tilde{S} = \sum_{j=1}^{M} e_j w_j \frac{\partial}{\partial n}\left[\sin\frac{\pi\eta}{2d}\cos k\xi\tau_1\right]_{(\eta,\xi)=(\eta(\theta_j),\xi(\theta_j))}\left(\frac{\mathrm{d}s}{\mathrm{d}\theta}\right)_{\theta=\theta_j}, \tag{27}$$

where $\{e_j\}$ is a normalized eigenfunction which corresponds to the eigenvalue of A which has smallest magnitude. Clearly $\tilde{S}$ is defined everywhere in the $(a/d, kd)$-plane and $\{e_j\}$ may be chosen so that $S = \tilde{S}$ on the line $\det(A) = 0$. The trapped mode is identified as the point where the line $\tilde{S} = 0$ crosses the line $\det(A) = 0$, provided that $\tilde{S}$ is real and varies smoothly in the vicinity of this point. (In principle $\tilde{S}$ could be complex if the eigenvalues of A with smallest magnitude are a complex conjugate pair, or $\tilde{S}$ could vary discontinuously if the lowest two eigenvalues of A change order.) However the identification of the line on which $\tilde{S} = 0$ requires the determination of the places at which $\tilde{S}$ changes sign and as $S = \tilde{S}$ on the line $\det(A) = 0$, the location of the point which corresponds to a trapped mode is equivalent to that obtained by using S directly. This technique for finding trapped modes is more robust numerically than that of looking for zeros of the complex determinant of the matrix which is obtained by discretizing (20) directly, because it is found that the curves on which the real and imaginary part of the determinant are zero touch rather than cross in the $(a/d, kd)$-plane.

In the next section an approximate trapped mode solution for a long plate on the centreline of the guide ($b/d = 0$, $a/d \gg 1$) is developed and in section 4 asymptotic expressions for the trapped mode parameters for slender bodies ($a/d \ll 1$) are obtained. The values of kd and the geometric parameters predicted for these approximate trapped modes will then be compared with the full numerical solutions in section 5.

3. A wide-spacing approximation for thin plates

For the case of a thin plate aligned with the waveguide we can derive an approximate solution based on the assumption that the plate is long compared to the wavelength, that is, $ka \gg 1$. (As kd is bounded this means that $a/d \gg 1$ also.) This technique was used by Evans (**12**) to investigate trapped modes below the continuous spectrum for exactly the same geometry. The basic idea is to assume that the two ends of the plate are sufficiently far apart so that the solution near to one of them is not affected by the other and then to utilize the fact that the scattering problem involving a semi-infinite thin plate can be solved explicitly.

More specifically, consider the three scattering problems illustrated schematically in Fig. 2. In each of the three pictures the heavier lines represent boundaries on which Neumann conditions are applied and the thin lines represent Dirichlet boundaries. Separation of variables shows that

solutions in $x < 0$ and $x > 0$ can be written as linear combinations of the terms $\exp(\pm k_n x)\psi_n(y)$, $n \geqslant 0$, and $\exp(\pm\kappa_n x)\Psi_n(y)$, $n \geqslant 1$, respectively, where

$$\psi_n(y) = \epsilon_n^{1/2} \cos \lambda_n y/d, \qquad k_n d = (\lambda_n^2 - k^2 d^2)^{1/2}, \qquad \lambda_n = n\pi, \tag{28}$$

$$\Psi_n(y) = 2^{1/2} \sin \mu_n y/d, \qquad \kappa_n d = (\mu_n^2 - k^2 d^2)^{1/2}, \qquad \mu_n = (n - \tfrac{1}{2})\pi, \tag{29}$$

and $\epsilon_0 = 1$, $\epsilon_n = 2$, $n \geqslant 1$. If we assume that the wave number kd lies in the range $\pi < kd < 3\pi/2$, then k_0, k_1 and κ_1 are purely imaginary whereas k_n, κ_n, $n \geqslant 2$, are real and we can define k, α and β (all real and positive) as follows:

$$k_0 d = -ikd, \quad k_1 d = -i(k^2 d^2 - \pi^2)^{1/2} = -i\alpha d, \quad \kappa_1 d = -i(k^2 d^2 - \pi^2/4)^{1/2} = -i\beta d. \tag{30}$$

Imaginary values of k_n and κ_n correspond to wave modes and so two such modes can exist in the region $x < 0$ whilst only one such mode is possible in $x > 0$. The two upper pictures illustrate scattering problems where the incident wave is one of the two possible modes that can approach from $x = -\infty$ and these problems can each be characterized by two reflection and one transmission coefficient. Both of these scattering problems can be solved explicitly using the residue calculus technique (see Mittra and Lee (**13**) for a detailed description of this technique), but before this is done we will show how the solutions can be related to trapped modes.

It is possible to construct a third scattering problem, illustrated in the lowest picture, by taking a linear combination of the first two in such a way that there are no waves as $x \to \infty$. In other words this third problem has the property that its solution decays to zero as $x \to \infty$. If we imagine a trapped mode in the vicinity of a long plate situated along $y = 0$, $-2a < x < 0$, then near to the right-hand end the solution would look like this third problem, with wave motion between the plate and the waveguide wall but no waves to the right of the plate. For the solution, ϕ, to this third problem to correspond to a trapped mode which is symmetric about the midpoint of the plate we would require $\partial\phi/\partial x = 0$ on $x = -a$, and this condition, together with the orthogonality of the set of functions $\{\psi_n(y)\}$ on $(0, y)$, gives rise to the two conditions

$$e^{-2ika} = R_0 - \frac{T_1 \widetilde{R}_0}{\widetilde{T}_1}, \tag{31}$$

$$e^{-2i\alpha a} = \widetilde{R}_1 - \frac{\widetilde{T}_1 R_1}{T_1}. \tag{32}$$

It can be shown, using judicious applications of Green's theorem, that the combinations of reflection and transmission coefficients that appear on the right-hand side of these conditions have unit modulus for all values of kd in the range $(\pi, 3\pi/2)$. The question is, can we find pairs of values $(a/d, kd)$ for which both (31) and (32) are satisfied simultaneously?

Whilst there is no guarantee that such an approximate solution corresponds to a trapped mode for the full problem, previous results suggest that the correspondence is extremely close, even for relatively small values of a/d, and moreover the wide-spacing approximation can be used as the basis for an existence proof for sufficiently large a/d (see the Appendix).

Let us examine in detail the solution of the problem illustrated uppermost in Fig. 2 and the determination of R_0, R_1 and T_1. In $x < 0$ we expand the solution, ϕ, as

$$\phi = (e^{-k_0 x} + e^{k_0 x})\psi_0(y) + \sum_{n=0}^{\infty} \frac{U_n^{(1)}}{k_n d}\, e^{k_n x}\, \psi_n(y), \tag{33}$$

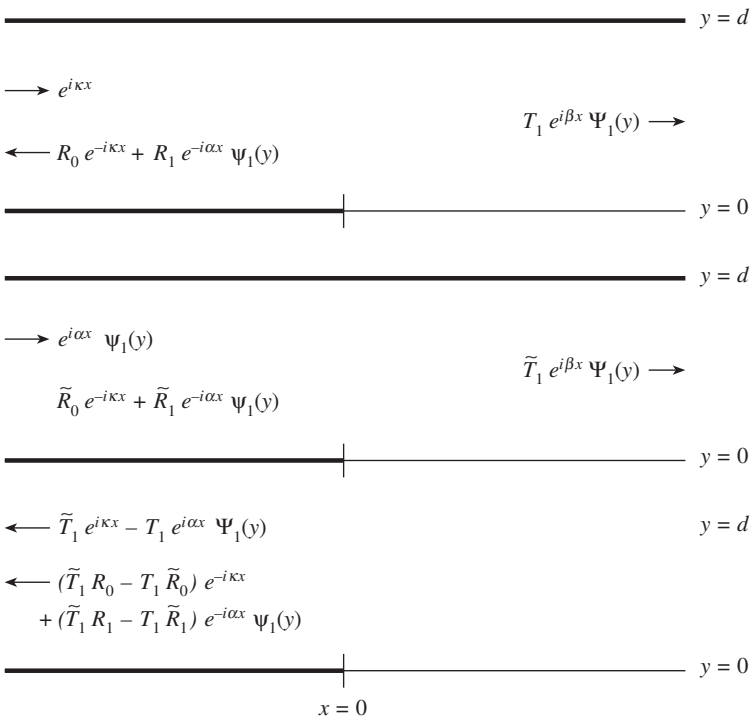

Fig. 2 Three scattering problems

where $U_n^{(1)}$, $n \geqslant 0$ are complex constants to be determined, $U_0^{(1)} = k_0 d(R_0 - 1)$ and $U_1^{(1)} = k_1 d R_1$. Similarly, in $x > 0$, we write

$$\phi = -\sum_{n=1}^{\infty} \frac{U_n^{(2)}}{\kappa_n d}\, e^{-\kappa_n x}\, \Psi_n(y) \tag{34}$$

with $U_1^{(2)} = -\kappa_1 d T_1$ and then we enforce continuity of ϕ and $\partial\phi/\partial x$ across $x = 0$. If we use the orthogonality of the functions ψ_n and then eliminate $U_n^{(1)}$ we obtain

$$\sum_{n=1}^{\infty} \frac{U_n}{\kappa_n d - k_m d} = -\delta_{0m}, \qquad m \geqslant 0, \tag{35}$$

where

$$U_n = \frac{U_n^{(2)} \mu_n}{\sqrt{2} k_0 d \kappa_n d}. \tag{36}$$

Note that the unknowns $U_n^{(2)}$ are the coefficients in the expansion of the horizontal velocity and so

we can determine their behaviour as $n \to \infty$. In order that the energy of the trapped mode is finite the form of the velocity at the end of the plate must be $\partial\phi/\partial r = O(r^{-1/2})$ as $r = (x^2+y^2)^{1/2} \to 0$, and it follows from the fact that for $0 < \nu < 1$

$$\sum_{n=1}^{\infty} n^{\nu-1}\, e^{-nx} \sim x^{-\nu}\Gamma(\nu) \quad \text{as} \quad x \to 0^+ \tag{37}$$

(see, for example, Martin (**14**)) that $U_n^{(2)} = O(n^{-1/2})$ as $n \to \infty$. The system of equations (35) is exactly the same as in Evans (**12**, equation (2.22)) (apart from the fact that here k_1 and κ_1 are imaginary, whereas in Evans (**12**) they were real) and hence we find that U_n is the residue of $f(z)$ at $z = \kappa_n d$ and $U_n^{(1)} = -\sqrt{2}k_0 d\, f(-k_n d)$, where

$$f(z) = h \prod_{m=1}^{\infty} \frac{1 - z/k_m d}{1 - z/\kappa_m d}, \qquad h = \prod_{m=1}^{\infty} \frac{1 - k_0/\kappa_m}{1 - k_0/k_m}. \tag{38}$$

The solution can be shown to have the approximate behaviour as $n \to \infty$ to model the singularity at the plate tip correctly. We thus obtain

$$R_0 = -h \prod_{m=1}^{\infty} \frac{1 + k_0/k_m}{1 + k_0/\kappa_m}, \tag{39}$$

$$R_1 = -\sqrt{2}\,\frac{k_0}{k_1} h \prod_{m=1}^{\infty} \frac{1 + k_1/k_m}{1 + k_1/\kappa_m}, \tag{40}$$

$$T_1 = \frac{2\sqrt{2}}{\pi}\, k_0 d\, \kappa_1 d\, (1 - \kappa_1/k_1) h \prod_{m=2}^{\infty} \frac{1 - \kappa_1/k_m}{1 - \kappa_1/\kappa_m}. \tag{41}$$

For the scattering problem involving $\widetilde{R}_0$, $\widetilde{R}_1$ and $\widetilde{T}_1$ the solution is expanded in $x < 0$ as

$$\phi = (e^{-k_1 x} + e^{k_1 x})\psi_1(y) + \sum_{n=0}^{\infty} \frac{\widetilde{U}_n^{(1)}}{k_n d}\; e^{k_n x}\, \psi_n(y), \tag{42}$$

where $\widetilde{U}_0^{(1)} = k_0 d \widetilde{R}_0$ and $\widetilde{U}_1^{(1)} = k_1 d(\widetilde{R}_1 - 1)$, whereas in $x > 0$ we write

$$\phi = -\sum_{n=1}^{\infty} \frac{\widetilde{U}_n^{(2)}}{\kappa_n d}\; e^{-\kappa_n x}\, \Psi_n(y) \tag{43}$$

with $\widetilde{U}_1^{(2)} = -\kappa_1 d \widetilde{T}_1$. If we impose continuity of ϕ and $\partial\phi/\partial x$ across $x = 0$ and then use the orthogonality of the functions ψ_n we obtain

$$2\delta_{m1} + \frac{\widetilde{U}_m^{(1)}}{k_m d} = -\sum_{n=1}^{\infty} \frac{\widetilde{U}_n^{(2)}}{\kappa_n d} c_{mn}, \qquad m \geqslant 0, \tag{44}$$

$$\widetilde{U}_m^{(1)} = \sum_{n=1}^{\infty} \widetilde{U}_n^{(2)} c_{mn}, \qquad m \geqslant 0, \tag{45}$$

where

$$c_{mn} = \frac{(2\epsilon_m)^{1/2}\mu_n}{\kappa_n^2 d^2 - k_m^2 d^2}. \tag{46}$$

The elimination of $\widetilde{U}_m^{(1)}$ between (44) and (45) results in the system of equations

$$\sum_{n=1}^{\infty} \frac{\widetilde{U}_n}{\kappa_n d - k_m d} = -\delta_{m1}, \qquad m \geqslant 0, \tag{47}$$

where

$$\widetilde{U}_n = \frac{\widetilde{U}_n^{(2)}\mu_n}{k_1 d \kappa_n d} \tag{48}$$

and again we must have $U_n = O(n^{-1/2})$ as $n \to \infty$.

The method of solution follows closely that in Evans (**12**). Consider the function

$$\widetilde{f}(z) = \widetilde{h}\,\frac{1 - z/k_0 d}{1 - z/\kappa_1 d} \prod_{m=2}^{\infty} \frac{1 - z/k_m d}{1 - z/\kappa_m d}, \qquad \text{where} \qquad \widetilde{h} = \frac{1 - k_1/\kappa_1}{1 - k_1/k_0} \prod_{m=2}^{\infty} \frac{1 - k_1/\kappa_m}{1 - k_1/k_m}, \tag{49}$$

and the integrals

$$I_m = \lim_{N\to\infty} \frac{1}{2\pi i} \int_{C_N} \frac{\widetilde{f}(z)}{z - k_m d}\,\mathrm{d}z, \qquad m \geqslant 0, \tag{50}$$

where C_N are circles centred on the origin with radius $(N - \frac{1}{4})\pi$. It can be shown that $\widetilde{f}(z) = O(z^{-1/2})$ as $|z| \to \infty$ on the circles C_N (details of how to do this can be found in Evans (**12**, Appendix A)), and hence it follows that $I_m = 0$. Cauchy's residue theorem then gives

$$\sum_{n=1}^{\infty} \frac{\mathrm{Res}(\widetilde{f} : \kappa_n d)}{\kappa_n d - k_m d} = -\delta_{m1}, \qquad m \geqslant 0. \tag{51}$$

A comparison of (47) and (51) shows that $\widetilde{U}_n = \mathrm{Res}(\widetilde{f} : \kappa_n d)$ and this can be shown to be $O(n^{-1/2})$ as $n \to \infty$. We thus obtain

$$\widetilde{T}_1 = -\frac{\widetilde{U}_1^{(2)}}{\kappa_1 d} = -\frac{2}{\pi} k_1 d\,\widetilde{U}_1 = \frac{2}{\pi}\,k_1 d\,\kappa_1 d\,(1 - \kappa_1/k_0)\widetilde{h} \prod_{m=2}^{\infty} \frac{1 - \kappa_1/k_m}{1 - \kappa_1/\kappa_m}. \tag{52}$$

To determine $\widetilde{R}_0$ and $\widetilde{R}_1$ we consider the integrals

$$\lim_{N\to\infty} \frac{1}{2\pi i} \int_{C_N} \frac{\widetilde{f}(z)}{z + k_m d}\,\mathrm{d}z, \qquad m \geqslant 0, \tag{53}$$

which are all zero, and hence

$$\sum_{n=1}^{\infty} \frac{\mathrm{Res}(\widetilde{f} : \kappa_n d)}{\kappa_n d + k_m d} = -\widetilde{f}(-k_m d), \qquad m \geqslant 0. \tag{54}$$

Now if we divide (45) by $k_m d$ and add the result to (44) we obtain

$$\delta_{m1} + \frac{\widetilde{U}_m^{(1)}}{k_m d} = \left(\frac{\epsilon_m}{2}\right)^{1/2} \frac{k_1}{k_m} \sum_{n=1}^{\infty} \frac{\widetilde{U}_n}{\kappa_n d + k_m d} = -\left(\frac{\epsilon_m}{2}\right)^{1/2} \frac{k_1}{k_m}\, \widetilde{f}(-k_m d), \tag{55}$$

using (54). Thus

$$\widetilde{R}_0 = \frac{\widetilde{U}_0^{(1)}}{k_0 d} = -\widetilde{h} \frac{\sqrt{2} k_1/k_0}{1 + k_0/\kappa_1} \prod_{m=2}^{\infty} \frac{1 + k_0/k_m}{1 + k_0/\kappa_m}, \tag{56}$$

$$\widetilde{R}_1 = \frac{\widetilde{U}_1^{(1)}}{k_1 d} + 1 = -\widetilde{h} \frac{1 + k_1/k_0}{1 + k_1/\kappa_1} \prod_{m=2}^{\infty} \frac{1 + k_1/k_m}{1 + k_1/\kappa_m}. \tag{57}$$

These solutions can then be substituted into the conditions for trapped modes, (31) and (32). Considerable simplification results and our final condition for trapped modes is that both equations

$$ka = (n + \tfrac{1}{2})\pi - \chi_1, \tag{58}$$

$$\alpha a = (m + \tfrac{1}{2})\pi - \chi_2, \tag{59}$$

where

$$\chi_1 = \sum_{m=2}^{\infty} \left(\tan^{-1} \frac{k}{\kappa_m} - \tan^{-1} \frac{k}{k_m} \right), \tag{60}$$

$$\chi_2 = \sum_{m=2}^{\infty} \left(\tan^{-1} \frac{\alpha}{\kappa_m} - \tan^{-1} \frac{\alpha}{k_m} \right) \tag{61}$$

are satisfied simultaneously, for an arbitrary pair of integers n and m.

The terms in the series in (60) and (61) are $O(m^{-2})$ as $m \to \infty$. For computational purposes we write

$$\chi_1 = \frac{k}{4\pi} \left(\frac{\pi^2}{3} - 3 + \zeta(3) \right) + \sum_{m=2}^{\infty} \left(\tan^{-1} \frac{k}{\kappa_m} - \tan^{-1} \frac{k}{k_m} - \frac{k(2m+1)}{4\pi m^3} \right), \tag{62}$$

$$\chi_2 = \frac{\alpha}{4\pi} \left(\frac{\pi^2}{3} - 3 + \zeta(3) \right) + \sum_{m=2}^{\infty} \left(\tan^{-1} \frac{\alpha}{\kappa_m} - \tan^{-1} \frac{\alpha}{k_m} - \frac{\alpha(2m+1)}{4\pi m^3} \right) \tag{63}$$

in which $\zeta(s)$ is the Riemann zeta function and the terms in the series are $O(m^{-4})$ as $m \to \infty$.

4. Wave trapping by a slender structure

In this section an asymptotic theory based upon the work of Evans and McIver (**15**) is developed for wave trapping by a slender structure. This allows the limiting behaviour to be calculated as the dimension of a structure measured in the direction along the channel tends to zero. In particular, it is shown for an ellipse $(x/a)^2 + (y/b)^2 = 1$ that as $a/d \to 0$ then $b/d \to B \approx 0{\cdot}392$. If the structure's width is much less than its depth then its surface in the first quadrant may be described

by $x = \epsilon f(y)$, $0 \leqslant y \leqslant d$, where $\epsilon \ll 1$. The slenderness assumption $\epsilon \ll 1$ allows equations (2), (3) to be replaced by

$$\phi = 0 \quad \text{on} \quad y = 0, \quad x > 0, \tag{64}$$

and

$$\frac{\partial \phi}{\partial y} = 0 \quad \text{on} \quad y = d, \quad x > 0, \tag{65}$$

respectively, and (5) and (4) to be replaced by

$$\frac{\partial \phi}{\partial x} = \epsilon(f'(y)\phi_y - f(y)\phi_{xx}) + O(\epsilon^2) \quad \text{on} \quad x = 0, \quad 0 < y < d. \tag{66}$$

The last equation is obtained by Taylor expansion about $x = 0$.

The functions $\Psi_n(y)$ and variables κ_n are defined in (29) and so for a trapped mode solution satisfying (6), separation of variables yields

$$\phi(x, y) = e^{-\kappa_2 x}\, \Psi_2(y) + \chi(x, y), \tag{67}$$

where

$$\chi(x, y) = \sum_{n=3}^{\infty} A_n\, e^{-\kappa_n x}\, \Psi_n(y) \tag{68}$$

and the term involving κ_1 has been omitted as it does not decay as $x \to \infty$. By construction, for all $x \geqslant 0$

$$\int_0^d \chi(x, y)\Psi_n(y)\, \mathrm{d}y = 0, \quad n = 1, 2. \tag{69}$$

It remains to satisfy the boundary condition (66). A solution for χ is sought in the form

$$\chi(x, y) = \chi_0(x, y) + \epsilon\chi_1(x, y) + O(\epsilon^2) \quad \text{as} \quad \epsilon \to 0, \tag{70}$$

where each χ_n is strictly of order unity in ϵ. Substitution of this expansion into (66) gives

$$\begin{aligned} &-\kappa_2\Psi_2(y) + \frac{\partial \chi_0}{\partial x}(0, y) + \epsilon\frac{\partial \chi_1}{\partial x}(0, y) \\ &\qquad = \epsilon\left\{ f'(y)\left(\Psi_2'(y) + \frac{\partial \chi_0}{\partial y}(0, y)\right) - f(y)\left(\kappa_2^2\Psi_2(y) + \frac{\partial^2 \chi_0}{\partial x^2}(0, y)\right)\right\} + O(\epsilon^2). \end{aligned} \tag{71}$$

Now if κ_2 is strictly of order one in ϵ then (71) gives

$$\frac{\partial \chi_0}{\partial x}(0, y) = \kappa_2\Psi_2(y), \quad 0 < y < d, \tag{72}$$

to leading order, which contradicts (69) with $n = 2$. Let $\kappa_2 = \epsilon^p\beta_2$, where p is a positive integer and β_2 is strictly of order one in ϵ. The leading-order terms in (71) then give

$$\frac{\partial \chi_0}{\partial x}(0, y) = 0, \quad 0 < y < d, \tag{73}$$

and so, after taking account of the other boundary conditions, it follows that $\chi_0(x, y) \equiv 0$. If $p > 1$, then to leading order

$$\frac{\partial \chi_1}{\partial x}(0, y) = f'(y)\Psi_2'(y), \quad 0 < y < d, \tag{74}$$

which contradicts (69) except possibly for special $f(y)$ that satisfy

$$\int_0^d f'(y)\Psi_2'(y)\Psi_n(y)\,\mathrm{d}y = 0, \quad n = 1, 2. \tag{75}$$

Under the assumption that both of these last conditions are not satisfied, it follows that $p = 1$ and at order ϵ equation (71) is

$$\frac{\partial \chi_1}{\partial x}(0, y) = \beta_2\Psi_2(y) + f'(y)\Psi_2'(y). \tag{76}$$

The conditions (69) then yield

$$\int_0^d f'(y)\Psi_2'(y)\Psi_1(y)\,\mathrm{d}y = 0 \tag{77}$$

and

$$\kappa_2 d = -\epsilon \int_0^d f'(y)\Psi_2'(y)\Psi_2(y)\,\mathrm{d}y. \tag{78}$$

It is now apparent that if equations (75) are satisfied, then this corresponds to trapped waves having frequencies within $o(\epsilon)$ of the cut-off as $\epsilon \to 0$. Equation (77) is the condition for the existence of a trapped mode and equation (78) determines the corresponding trapped mode frequency.

The shape function

$$x = \epsilon f(y) \equiv a\left(1 - \frac{y^2}{b^2}\right)^{1/2}, \quad b \leqslant d, \tag{79}$$

describes an ellipse of axes length $2a$ in the x-direction and $2b$ in the y-direction. The integrations in (77) may be carried out using a result given by Gradshteyn and Ryzhik (**16**, equation 3.753:5) and it is found that trapped modes exist whenever b/d is a solution of

$$J_1(2\pi b/d) - J_1(\pi b/d) = 0, \tag{80}$$

where J_1 denotes the first-kind Bessel function of order one. This equation has only one root

$$b/d = B \approx 0{\cdot}392 \tag{81}$$

for $0 < b/d \leqslant 1$. The corresponding trapped mode frequency follows from (78) and for this geometry

$$kd = \frac{3\pi}{2} - \frac{3\pi^3 a^2}{16d^2}[J_1(3\pi B)]^2 + O(a^4/d^4) \quad \text{as} \quad a/d \to 0. \tag{82}$$

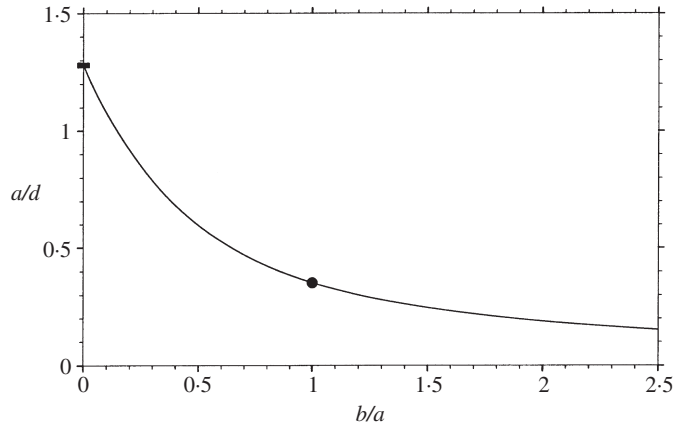

Fig. 3 Sizes and aspect ratios of elliptical obstacles that are able to support trapped modes; • circle; ▬ parallel plate; ——: numerical values

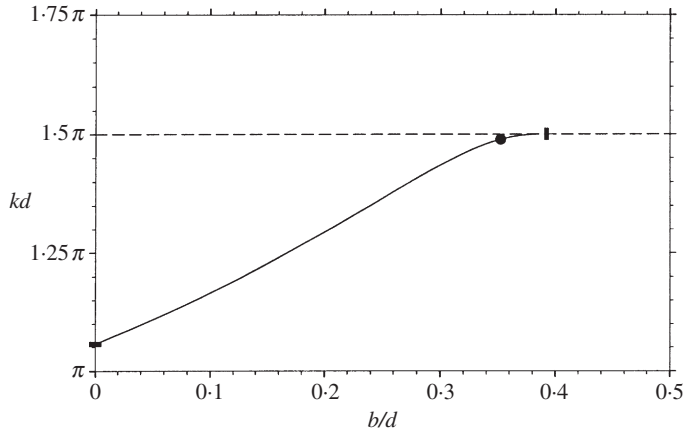

Fig. 4 Wave numbers of trapped modes supported by ellipses, as a function of b/d; • circle; ▬ parallel plate; ▌perpendicular plate; ——: numerical values; - - -: $kd = 3\pi/2$

5. Results and discussion

Figure 3 illustrates the sizes and aspect ratios of the elliptical obstacles which support embedded trapped modes and Figs 4 and 5 give the corresponding values of kd as functions of b/d and a/d respectively. Evans and Porter (**7**) showed numerically that an embedded trapped mode exists for the special case of a circle with radius $a/d = b/d \approx 0{\cdot}352$ at a wave number $kd \approx 1{\cdot}489\pi$. This point is indicated on each of the three figures by a solid circle. The values of a/d and kd for the plate on the centreline are calculated from (58) and (59) with $n = 1$ and $m = 0$. This trapped

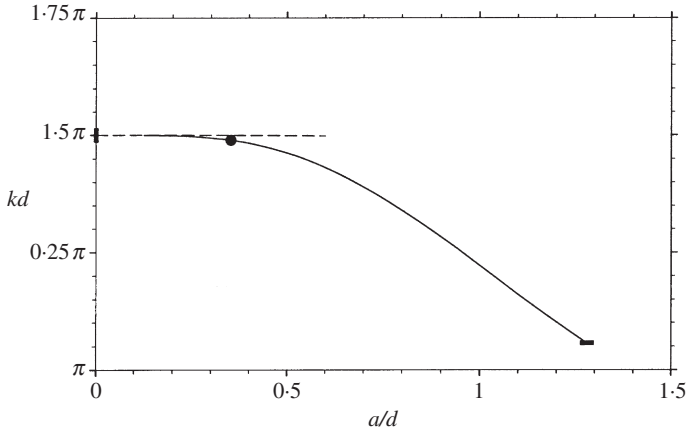

Fig. 5 Wave numbers of trapped modes supported by ellipses, as a function of a/d; • circle; ▬ parallel plate; ▌perpendicular plate; ——: numerical values; - - -: slender body approximation

mode is indicated by a horizontal bar on each of the figures and it forms the end point of each of the curves, where $b/d = 0$. In the other limit when the plate becomes perpendicular to the guide walls, that is $a/d \to 0$, the limiting value of b/d is given by B as defined in (81). This point is indicated by a vertical bar on the figures. The limiting form of kd is given by (82) and is drawn as a dashed line in Fig. 5. The remaining points in the figures are obtained from the numerical scheme described in section 2.

The figures corroborate the findings of Evans and Porter (**7**) that an embedded trapped mode exists for a circle and give strong evidence that this mode is not isolated but is a point on a continuous branch of modes for ellipses of varying aspect ratio. From Fig. 4, $kd < 3\pi/2$ for the plate on the centreline ($b/d = 0$) and so this plate can support a trapped mode. However from Fig. 5, $kd = 3\pi/2$ for the plate perpendicular to the guide walls ($a/d = 0$) and so this limiting point does not correspond to a genuine trapped mode. Instead the limiting form of the motion is the standing wave $\sin 3\pi y/2d$, which does not decay as $x \to \infty$. Thus the branch starts with a trapped mode for a thin plate on the centreline and terminates with a standing wave for a thin plate perpendicular to the walls.

The embedded trapped mode for a circle was also found numerically to be a point on a branch of modes for obstacles with shapes of the form $|x/a|^\nu + |y/a|^\nu = 1$, $1 \leqslant \nu < \infty$, the circle corresponding to $\nu = 2$. Figure 6 gives the values of a/d for which trapped modes exist as a function of ν and Fig. 7 shows the shape and size of the obstacle for different values of ν. The corresponding trapped mode wave numbers are presented in Fig. 8. The trapped mode parameter values for the circle are again designated by solid circles. As $\nu \to \infty$ the shape tends to a square with sides of half-length $a/d = \frac{1}{3}$ and the trapped mode tends to the standing wave $\sin 3\pi y/2d$ as this standing wave satisfies the boundary conditions exactly on the square. Numerical difficulties meant that the calculations could not be made easily for values of ν less than about 1, but theoretically ν may be decreased to 0 if the trapped mode is considered to be a mode in a semi-infinite guide with a variably shaped end, once the body touches the guide.

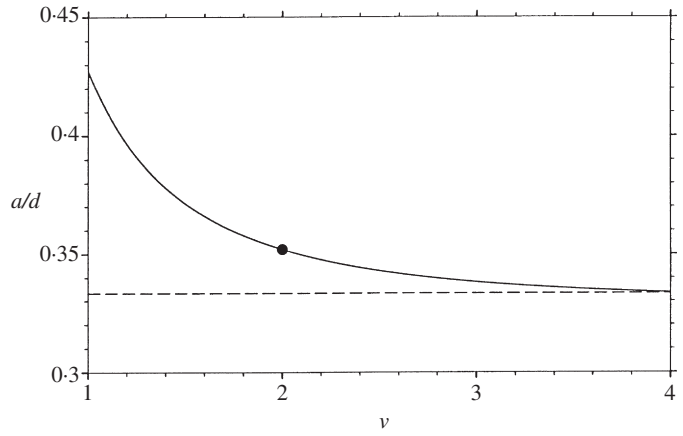

Fig. 6 Values of a/d for shapes $|x/a|^\nu + |y/a|^\nu = 1$ which are able to support trapped modes, as a function of ν; • circle; ——: numerical values; - - -: $a/d = 1/3$

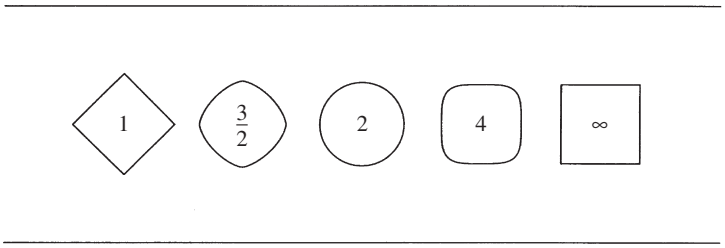

Fig. 7 Shapes and sizes of the obstacles $|x/a|^\nu + |y/a|^\nu = 1$ which are able to support trapped modes or in the case of a square, a standing wave; values of ν are marked on bodies

Calculations reveal that (58) and (59) possess infinitely many solutions corresponding to different combinations of m and n ($m < n$). All these other solutions correspond to longer plate lengths than the one that appears in the figures and in fact $a/d \to \infty$ as $n \to \infty$. These geometries form the end points of further branches of ellipses for which trapped modes exist. However, there is nothing special about elliptical obstacles and these plates may be continuously deformed into obstacles of other shapes, for example rectangular blocks. An extensive investigation into the higher branch structure for embedded trapped modes for rectangular blocks will form the subject of a further paper. The rectangular block has the interesting property that the function $\sin 3\pi y/2d$ corresponds to a standing wave for *any* block with $b/d = \frac{1}{3}$ irrespective of its length. This important property has significant consequences for the behaviour of the higher branches of trapped modes which will be investigated in detail in the subsequent paper.

A further natural question to ask is whether any embedded trapped modes exist at wave numbers above the next cut-off for antisymmetric wave propagation. In general one would expect to have

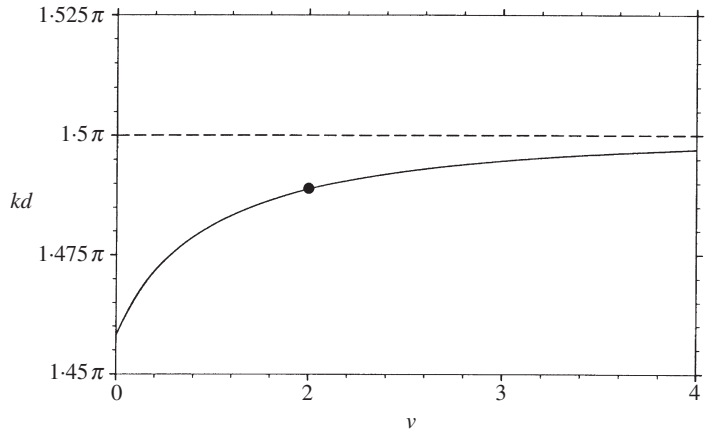

Fig. 8 Wave numbers of trapped modes supported by shapes $|x/a|^\nu + |y/a|^\nu = 1$; • circle; ——: numerical values; - - -: $kd = 3\pi/2$

to vary an additional geometrical parameter every time a new cut-off is exceeded in order to obtain a trapped mode. This is because an extra wave-like term appears in the Green's function at every cut-off and this leads to an additional side condition which needs to be satisfied. If the body has no symmetry in x then two extra side conditions need to be satisfied every time a new cut-off is passed which means that two additional geometric parameters must be varied in order to obtain a trapped mode. Thus trapped modes are expected to become rarer as the wave number increases, and unstable to more classes of geometric perturbations. For example it is possible that there is a countable number of ellipses with semi-major and semi-minor axes of specific lengths for which a trapped mode exists if kd is restricted to the range $3\pi/2 < kd < 5\pi/2$. This is compared with the fact that all ellipses support trapped modes when $kd < \pi/2$ and in this work, continuous branches of ellipses were found to support trapped modes when kd is restricted to the range $\pi/2 < kd < 3\pi/2$.

Acknowledgements

The work of the fourth author was supported by EPSRC grant GR/M30937

References

1. D. V. Evans, M. Levitin and D. Vassiliev, Existence theorems for trapped modes, *J. Fluid Mech.* **261** (1994) 21–31.
2. N. S. A. Khallaf, L. Parnovski and D. Vassiliev, Trapped modes in a waveguide with a long obstacle, *Ibid.* **403** (2000) 251–261.
3. D. V. Evans, C. M. Linton and F. Ursell, Trapped mode frequencies embedded in the continuous spectrum, *Q. Jl Mech. Appl. Math.* **46** (1993) 253–274.
4. E. B. Davies and L. Parnovski, Trapped modes in acoustic waveguides, *Ibid.* **51** (1998) 477–492.

5. M. D. Groves, Examples of embedded eigenvalues for problems in acoustic waveguides, *Math. Meth. Appl. Scis* **21** (1998) 479–488.
6. C. M. Linton and M. McIver, Trapped modes in cylindrical waveguides, *Q. Jl Mech. Appl. Math.* **51** (1998) 389–412.
7. D. V. Evans and R. Porter, Trapped modes embedded in the continuous spectrum, *Ibid.* **52** (1998) 263–274.
8. C. M. Linton and D. V. Evans, Integral equations for a class of problems concerning obstacles in waveguides, *J. Fluid Mech.* **245** (1992) 349–365.
9. R. Courant and D. Hilbert, *Methods of Mathematical Physics*, Vol. 1 (Interscience, New York 1953).
10. M. Abramowitz and I. A. Stegun, *Handbook of Mathematical Functions* (Dover, New York 1965).
11. C. M. Linton, The Green's function for the two-dimensional Helmholtz equation in periodic domains, *J. Eng. Math.* **33** (1998) 377–402.
12. D. V. Evans, Trapped acoustic modes, *IMA J. Appl. Math.* **49** (1992) 45–60.
13. R. Mittra and S. W. Lee, *Analytical Techniques in the Theory of Guided Waves* (Macmillan, New York 1971).
14. P. A. Martin, Asymptotic approximations for functions defined by series, with some applications in the theory of guided waves, *IMA J. Appl. Math.* **54** (1995) 139–157.
15. D. V. Evans and P. McIver, Trapped waves over symmetric thin bodies, *J. Fluid Mech.* **223** (1991) 509–519.
16. I. S. Gradshteyn and I. M. Ryzhik, *Tables of Integrals, Series and Products* (Academic Press, New York 1965).
17. V. Hutson and J. S. Pym, *Applications of Functional Analysis and Operator Theory* (Academic Press, London 1980).

APPENDIX

Existence proof for long plates

The method used in section 3 can be extended to form an existence proof for trapped modes in the presence of a plate which is aligned with the guide walls. The procedure is very similar to that described in Evans (**12**) and allows us to prove that there is a countably infinite set of plates for which trapped modes exist provided that a/d is sufficiently large for each plate. As before we assume $\pi < kd < 3\pi/2$ and define $\psi_n(y)$, k_n, λ_n, $\Psi_n(y)$, κ_n and μ_n by (28) and (29).

The geometry is as shown in Fig. 1, with $b = 0$. In $0 < x < a$ we expand the solution, ϕ, as

$$\phi = \sum_{n=0}^{\infty} U_n^{(1)} \frac{\cosh k_n x}{k_n d \sinh k_n a} \psi_n(y) \tag{A1}$$

and in $x > a$ we write

$$\phi = -\sum_{n=2}^{\infty} U_n^{(2)} \frac{e^{-\kappa_n(x-a)}}{\kappa_n d} \Psi_n(y). \tag{A2}$$

Note that the summation here starts from $n = 2$ so that $\phi \to 0$ as $x \to \infty$. If we then impose continuity of ϕ and $\partial\phi/\partial x$ across $x = a$ and eliminate $U_n^{(1)}$ we obtain the infinite system of equations

$$\sum_{n=2}^{\infty} U_n \left(\frac{1}{\kappa_n d - k_m d} + \frac{e^{-2k_m a}}{\kappa_n d + k_m d} \right) = 0, \qquad m \geqslant 0, \tag{A3}$$

where $U_n = \mu_n U_n^{(2)}/\kappa_n$.

To solve this system we write $f(z) = h(z)g(z)$, where

$$g(z) = \prod_{n=2}^{\infty} \frac{1 - z/k_n d}{1 - z/\kappa_n d}, \qquad h(z) = 1 + \sum_{n=2}^{\infty} \frac{A_n}{zd - k_n d}, \tag{A4}$$

the coefficients A_n being undetermined, and consider the integrals

$$I_m = \lim_{N\to\infty} \frac{1}{2\pi i} \int_{C_N} f(z) \left(\frac{1}{z - k_m d} + \frac{e^{-2k_m a}}{z + k_m d} \right) \mathrm{d}z \qquad m \geqslant 0, \tag{A5}$$

where C_N are circles centred on the origin with radius $(N - \frac{1}{4})\pi$. Since $g(z) = O(z^{-1/2})$ as $|z| \to \infty$ on the circles C_N (see, Evans (**12**, Appendix A)), we have $I_m = 0$. Cauchy's residue theorem then gives

$$\sum_{n=2}^{\infty} \mathrm{Res}(f : \kappa_n d) \left(\frac{1}{\kappa_n d - k_m d} + \frac{e^{-2k_m a}}{\kappa_n d + k_m d} \right) + f(k_m d) + e^{-2k_m a} f(-k_m d) = 0, \qquad m \geqslant 0. \tag{A6}$$

Thus U_n is given by the residue of $f(z)$ at $z = \kappa_n d$ provided

$$f(k_m d) + e^{-2k_m a} f(-k_m d) = 0, \qquad m \geqslant 0 \tag{A7}$$

and it follows (see, Evans (**12**, Appendix C)) that $U_n = O(n^{-1/2})$ as $n \to \infty$. This in turn implies that $\partial\phi/\partial r = r^{-1/2}$ as $r = [(x - a)^2 + y^2]^{1/2} \to 0$ which shows that our solution has the correct behaviour near the end of the plate.

We begin by considering (A7) with $m \geqslant 2$. These equations are solved if the coefficients A_m which appear in (A4) are the solutions to the infinite systems of real equations

$$A_m + D_m \sum_{n=2}^{\infty} \frac{A_n}{k_m d + k_n d} = D_m, \qquad m \geqslant 2, \tag{A8}$$

where

$$D_m = \frac{2k_m d(\kappa_m - k_m)}{(\kappa_m + k_m)} \, e^{-2k_m a} \prod_{\substack{n=2 \\ n\neq m}}^{\infty} \frac{(1 - k_m/\kappa_n)(1 + k_m/k_n)}{(1 + k_m/\kappa_n)(1 - k_m/k_n)}. \tag{A9}$$

Because of the presence of the factor $e^{-2k_m a}$ in the expression for D_m, the system of equations (A8) converges very quickly provided a/d is not too small. A sufficient condition for the infinite system to possess a unique solution A_n, with $\sum_{n=1}^{\infty} A_n^2 < \infty$, is that $\sum_{n=1}^{\infty} D_n^2 < \infty$ and $\sum \sum_{n,m=1}^{\infty} D_m^2/(k_m d + k_n d)^2 < 1$ (see, for example, Hutson and Pym (**17**, section 3.6)). That these inequalities are satisfied, provided a/d is sufficiently large, is easily proved (only minor modifications to the argument of Evans (**12**, Appendix B), are required).

It remains to satisfy (A7) for $m = 0$ and 1. Thus the condition for trapped modes is that both equations

$$ka = (n + \tfrac{1}{2})\pi - \chi_1 + \delta_1, \tag{A10}$$

$$\alpha a = (m + \tfrac{1}{2})\pi - \chi_2 + \delta_2, \tag{A11}$$

where χ_1 and χ_2 are defined in (60) and (61), and

$$\delta_1 = \arg\left(1 - \sum_{m=2}^{\infty} \frac{A_m}{ik + k_m} \right), \qquad \delta_2 = \arg\left(1 - \sum_{m=2}^{\infty} \frac{A_m}{i\alpha + k_m} \right) \tag{A12}$$

are satisfied simultaneously, for an arbitrary pair of integers n and m.

Now, as $a/d \to \infty$, $D_m \to 0$ and hence, from (A8), $A_m \to 0$ and then from (A12) $\delta_i \to 0$, $i = 1, 2$. Thus in this limit we recover the approximate conditions (58) and (59). Moreover, given any $\epsilon > 0$, we can choose a/d sufficiently large so that $\max(|\delta_1|, |\delta_2|) < \epsilon$. From (60), (61) and the fact that $\kappa_n < k_n < \kappa_{n+1}$, $n = 2, 3, \ldots$, we easily deduce that

$$0 < \chi_1 < \tan^{-1}(k/\kappa_1) < \pi/2, \qquad 0 < \chi_2 < \tan^{-1}(\alpha/\kappa_1) < \pi/2 \tag{A13}$$

and so if we define $c_1 = \pi/2 - \chi_1 + \delta_1$ and $c_2 = \pi/2 - \chi_2 + \delta_2$, then we can choose a/d sufficiently large so that $0 < c_1 < \pi/2$ and $0 < c_2 < \pi/2$. If we eliminate a from equations (A10) and (A11) we obtain

$$\frac{\alpha n\pi}{k} - m\pi = c_2 - \frac{\alpha c_1}{k} \tag{A14}$$

and we note that from (A10), since $\pi < kd < 3\pi/2$, the condition a/d sufficiently large is equivalent to the condition n sufficiently large.

As kd varies between π and $3\pi/2$, α/k varies continuously between 0 and $\sqrt{5}/3$ and so the left-hand side of this equation varies between $-m\pi$ and $(\sqrt{5}n/3 - m)\pi$ whilst, provided n is sufficiently large, the right-hand side varies continuously and always lies in the range $(-\pi/2, \pi/2)$. It follows that if we fix $m \geqslant 1$, we can always choose n large enough so that the infinite system of equations (A8) has a unique solution, both c_1 and c_2 lie in the range $(0, \pi/2)$ and $\sqrt{5}n/3 - m > \frac{1}{2}$. It then follows that there must be at least one value of kd in the range $(\pi, 3\pi/2)$ for which (A14) is satisfied. The corresponding value of a/d is then given by (A10).